Cumhuriyet Sci. J., 46(4) (2025) 911-916
DOI: https://doi.org/10.17776/csj.1737885

Cumhuriyet Science Journal

| csj.cumhuriyet.edu.tr | Founded: 2002 ISSN: 2587-2680 e-ISSN: 2587-246X Publisher: Sivas Cumhuriyet University

Gamma Attenuation Properties of $Li_2B_4O_7$ Doped with Gd

Hakan EROĞLU[1, a,*], Sümeyye Gümüş Uzun[1,b], Bayram Bilmez[2,c], Mustafa Çağatay Tufan[1,d], Mevlüt GÜRBÜZ[3,e], Bilgehan Cem Turan[3,f]

[1]*Ondokuz Mayis University, Graduate School, Department of Radiological Sciences, 55139 Atakum, Samsun*

[2]*Ondokuz Mayis University, Faculty of Sciences, Department of Physics, 55139 Atakum, Samsun*

[3]*Ondokuz Mayis University, Faculty of Engineering, Department of Mechanical Engineering, 55139 Atakum, Samsun*

**Corresponding author*

Research Article

History
Received: 31/07/2025
Accepted: 16/09/2025

ABSTRACT

In this study, the gamma attenuation properties of pure Li2B4O7 and 1 % mol Gd-doped Li2B4O7 were investigated using a gamma spectrometry system with narrow beam geometry. Samples were synthesized by the solid state reaction method. In the experimental part of the study, linear and mass attenuation coefficients were determined for 0.1218 MeV, 0.2447 MeV, 0.3443 MeV, 0.7789 MeV, 0.964 MeV, and 1.408 MeV energy peaks of Eu-152. The atomic and electronic cross sections, effective atomic number, and electron density, half value thickness (HVL), tenth value thickness (TVL), and mean free path (MFP) values were also calculated from these values. The obtained values were compared with XCOM values for theoretical data. It was found that Gd doping increased the attenuation coefficients in the low-energy region. However, its effects were limited at higher photon energies.

Keywords : Gamma attenuation coefficient, NaI(Tl) scintillation detector, Lithium tetra borate, Rare earth element

[a] *hakaneroglu55@gmail.com* *https://orcid.org/0009-0004-4072-1846*
[b] *sumeyye-gumus@hotmail.com* *https://orcid.org/0000-0003-1763-2373*
[c] *bayram.bilmez@omu.edu.tr* *https://orcid.org/0000-0002-5687-2145*
[d] *mctufan@omu.edu.tr* *https://orcid.org/0000-0003-3110-5115*
[e] *mgurbuz@omu.edu.tr* *https://orcid.org/0000-0003-2365-5918*

Introduction

With the increasing use of ionizing radiation in many different areas, from industry to science, determining the absorption properties of materials for this radiation has become the subject of many scientific studies. In particular, knowing the degree to which the intensity of the electromagnetic radiation beam is attenuated by matter is extremely important in terms of radiation protection and safe use of radiation. For this purpose, in addition to the linear and mass attenuation coefficients (μ, μm) of substances for ionizing electromagnetic radiation, their atomic and electronic cross sections (σt,a and σt,e), effective atomic number and electron densities (Zeff and Neff) must also be known. These properties vary according to the substance composition and the energy of the electromagnetic radiation.

Lithium tetraborate is typically observed as a white, crystalline solid or powder. It is well-known for its pyroelectric and piezoelectric properties [1-3], and its tetragonal crystal structure [4]. It is widely used in various scientific and industrial applications, such as a component in optical materials. The boron content in lithium tetraborate enables its application as a neutron shielding material in nuclear technology. On the other hand, it is also reported that Li2B4O7 is insensitive to γ-ray radiation with respect to neutron shielding [5].

Lanthanides are rare earth elements whose chemical properties are characterized by an unfilled 4f Shell [6]. These elements have various practical applications, from scintilators to optical devices [7]. These elements have been commonly used as a dopant to improve the luminescence properties of the materials [6, 8-12]. As a rare earth element, Gadolinium (Gd) has several applications in the nuclear industry and medicine [13-15].

This study investigated gamma attenuation properties of lithium tetraborate (Li2B4O7) and Li2B4O7 doped with 1% mol Gd. In this manner, linear and mass attenuation coefficients were determined using the well-known exponential attenuation law.

MATERIALS and METHODS

Preparation of the samples

In this study, pure and 1 mol% Gd-doped $Li_2B_4O_7$ samples were prepared using the solid-state synthesis method. Samples were prepared by mixing commercial powder forms of these elements using stoichiometric ratios. These powders were placed in the grinding chamber with 50 mL of ethyl alcohol and zirconium balls (50 balls were used, each one was 1 g) to obtain a homogeneous dissolution, and then left in the mill, rotated at 150 rpm for 24 h. Then, the materials were dried in a 70 °C oven for 20 h. Dried materials were crushed in an agate mortar and sieved. The materials were placed in the oven at 900 °C for two hours with a heating

rate of 5 °C/m. After the first heat treatment, the materials were crushed and sieved again. Powder samples were pressed under high pressure to obtain pellets. Pellets have square shapes, and thickness is 0.35 cm for $Li_2B_4O_7$ and 0.34 cm for $Li_2B_4O_7$:1%Gd. These steps are shown in Fig.1.

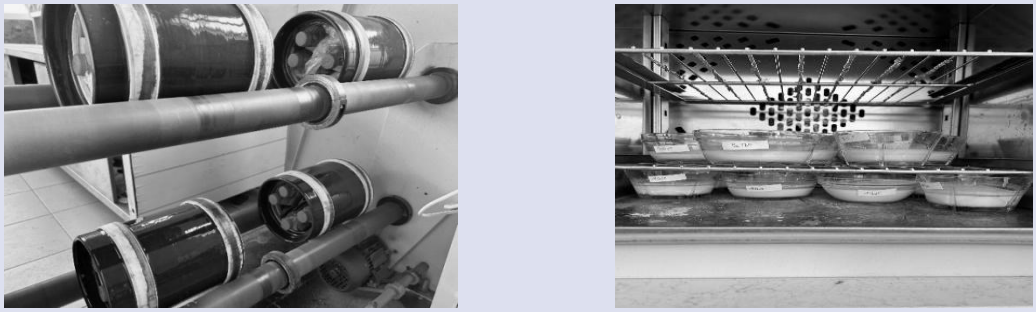

(A) (B)

Figure 1. (a) Mixing of grinding chambers in the mill, (b) Materials left to dry in the oven.

Theoretical background

Radiation attenuation refers to the reduction in radiation intensity as it passes through a material. Materials' response to the incident radiation depends on the type and energy of the incident radiation. In this work, gamma attenuation properties have been investigated, so that a well-known exponential attenuation law was used to determine the materials' properties [16-19]:

$$I=I0\ \exp(-\mu x.) \quad (1)$$

Here μ is the mass attenuation coefficient of the medium and is commonly used in the literature as a macroscopic cross-section and calculated as the ratio of the linear attenuation coefficient to the density of the medium (ρ):

$$\mu_m = \frac{\mu}{\rho} \quad (2)$$

Once linear and mass attenuation coefficients are determined, other important parameters for the determination of the material's gamma attenuation properties are calculated as follows:

for atomic and electronic cross sections [20]

$$\sigma_{t,a} = \frac{\mu_m}{N_A \sum_i \frac{\omega_i}{A_i}} \quad (3)$$

And

$$\sigma_{t,e} = \frac{1}{N_A} \sum \frac{f_i A_i}{Z_i} (\mu_m)_i \quad (4)$$

for effective atomic number (Zeff) [21]

$$Z_{eff} = \frac{\sigma_{t,a}}{\sigma_{t,e}} \quad (5)$$

and effective electron number (Neff) [20]

$$N_{eff} = \frac{\mu_m}{\sigma_{t,e}} \quad (6)$$

In the above equations, NA is Avogadro's constant, fi, Ai, and Zi are the number of ith elements relative to the total number of atoms of all elements in the mixture, atomic weights (in grams), and atomic number of the ith element.

Besides, the half-value layer (HVL) and tenth-value layer (TVL) are also important quantities. These represent the medium thicknesses at which the incident photons are attenuated to half and one-tenth of their initial intensity, respectively.

$$HVL = \frac{0{,}693}{\mu} \quad (7)$$

$$TVL = \frac{2{,}3026}{\mu} \quad (8)$$

As a measure of the penetration power of a photon beam before it interacts, the Mean Free Path (MFP) is used. It is equal to the thickness that reduces the incoming radiation to 1/e of the incident intensity. For mono-energetic photons, the MFP is

$$MFP = \frac{1}{\mu} \quad (9)$$

Experimental Setup

A NaI(Tl) scintillation detector with a digital signal processing unit (ORTEC-905-4) was used to perform the gamma spectrometric measurements. The detector yield is 2% at 0.5 MeV and 1.3% at 2 MeV. The detector was calibrated using the Eu-152 standard source. Since the system geometry and environment were not changed during the measurement, the background correction was performed using the trapezoidal method. The experimental setup is shown in Fig.1. Liquid Eu-152 has been used as a radioactivity source. The gamma rays corresponding to the energies 0.1218 MeV, 0.2447 MeV, 0.3443 MeV, 0.7789 MeV, 0.964 MeV, and 1.408 MeV were utilized in this study

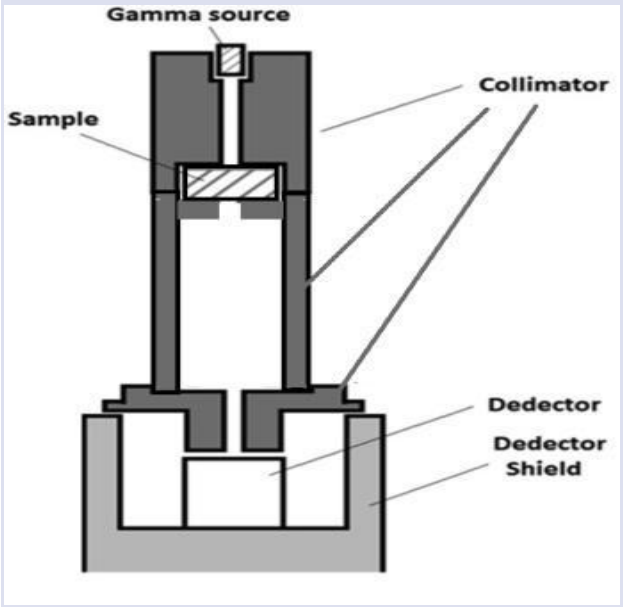

Figure 2. The experimental setup with NaI(Tl) scintillation detector, Eu-152 radioactive source and narrow beam collimators.

Results and Discussion

Densities of the samples were determined by applying Archimedes' principle: pure water was used for this, and the weight of the sample and the buoyancy force in water were measured. Table 1 shows the densities of the samples.

Table 1. Densities of samples

Sample	Density (g/cm^3)
$Li_2B_4O_7$	1.61 ± 0.00066394
$Li_2B_4O_7$: 1%Gd	1.58 ± 0.00067546

Linear attenuation coefficients of the samples were determined by measuring the radiation intensities of the gamma source with (I) and without (I_0) the sample and using these intensities in Eq.1. Linear and mass attenuation coefficients are shown together with the NIST XCOM values [22] in Table 2. These values have been plotted and shown in Fig.3. Mass attenuation coefficients of the samples have been also compared with each other in Fig.4.

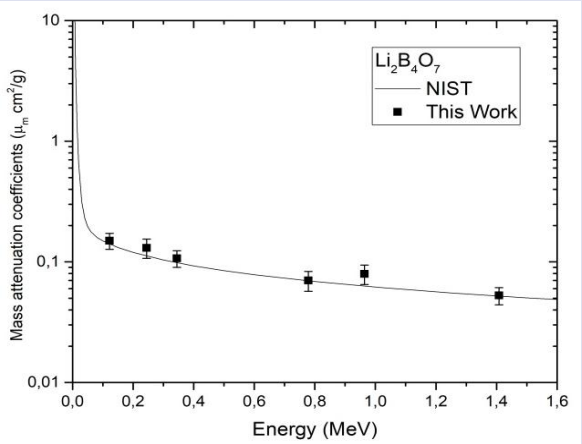

(a)

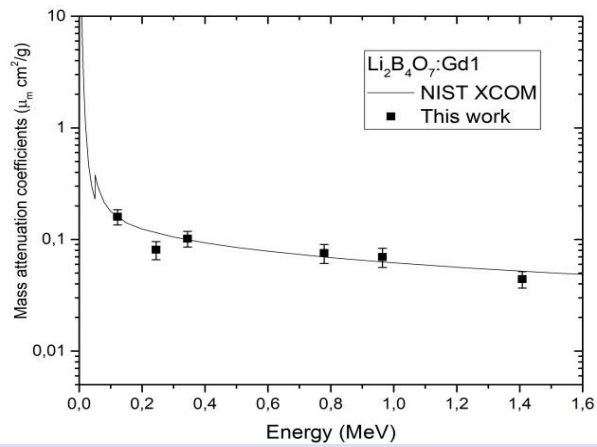

(b)

Figure 3. Mass attenuation coefficients for (a) Li2B4O7, (b) Li2B4O7:Gd1, in the energy range of 0.001 MeV to 3 MeV for XCOM values and experimental values corresponding to Eu-152 gamma energies.

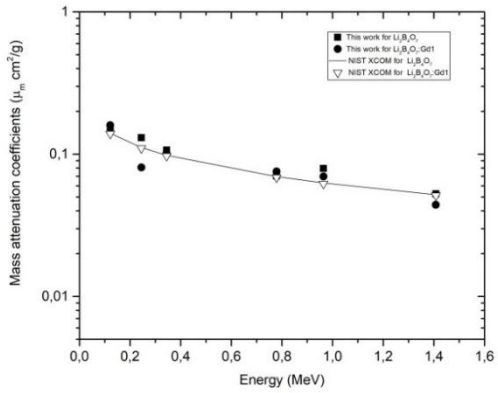

Figure 4. Comparison of mass attenuation coefficients

Table 2. experimental linear and mass attenuation coefficients of the samples and theoretical mass attenuation coefficients from the xcom database.

$Li_2B_4O_7$			
Energy (MeV)	**μ (1/cm)**	**μm (cm2/g)**	**NIST XCOM μm (cm2/g)**
0.1218	0.24096±0.0367	0.14967±0.02286	0.1402
0.2447	0.21041±0.03806	0.13069±0.02369	0.1116
0.3443	0.17224±0.02711	0.10698±0.01688	0.09833
0.7789	0.11299±0.02099	0.07018±0.01307	0.06956
0.964	0.12801±0.02334	0.07951±0.01453	0.06288
1.408	0.08475±0.01378	0.05264±0.00858	0.05194
	Li2B4O7: 1%Gd		
Energy (MeV)	**μ (1/cm)**	**μm (cm2/g)**	**NIST XCOM μm (cm2/g)**
0.1218	0.25278±0.03972	0.15999±0.02521	0.1392
0.2447	0.12762±0.02353	0.08077±0.01492	0.1102
0.3443	0.16082±0.02578	0.10179±0.01636	0.09699
0.7789	0.11945±0.02299	0.0756 ±0.01458	0.06858
0.964	0.11023±0.02141	0.06977 ±0.01358	0.06199
1.408	0.06967±0.01164	0.0441±0.00739	0.05121

We also show mass attenuation coefficients in Fig.2, along with the XCOM data, and propagated errors in the graphs. The uncertainties in the calculated values have been obtained from the relative errors of the measured values, which known as propagation of uncertainty method. As shown, the obtained results are in close agreement with the XCOM data.

In the case of undoped $Li_2B_4O_7$, the experimental data show a decreasing trend with increasing photon energy, consistent with the theoretical behaviour predicted by NIST. However, small deviations between experimental and theoretical values are observed, especially at around 0.964 MeV photon energies, where the experimental attenuation coefficients appear noticeably higher than the NIST values. These differences can be explained by experimental uncertainties, structural inhomogeneities, or the specific crystalline nature of the sample used.

For the Gd-doped sample, the mass attenuation coefficients are consistently higher than those of the pure $Li_2B_4O_7$ at lower photon energies (< 0.3 MeV), which can stem from the fact that the photoelectric effect is more dominant in this region. The presence of gadolinium (Z = 64), a high atomic number element compared with the rest of the constituents of the sample (with Z<10), significantly enhances photon interaction probability, especially via photoelectric absorption in low energy region.

At higher photon energies (> 1 MeV), the attenuation coefficients of both samples converge and show reduced differences. This behavior is expected, as Compton scattering dominates in this energy range.

In addition to the experimentally determined mass attenuation coefficients, several photon interaction parameters were calculated for both pure and Gd-doped $Li_2B_4O_7$ samples over a range of photon energies (0.1218–1.408 MeV). These parameters include the effective atomic number (Zeff), effective electron density (Neff), microscopic cross-sections (σa and σe), as well as shielding parameters such as half value layer (HVL), tenth value layer (TVL), and mean free path (MFP). The detailed results are provided in Table 3.

Table 3. Gamma interaction parameters of the samples.

$Li_2B_4O_7$							
Enerji (MeV)	σ_a	σ_e	Z_{eff}	N_{eff}	HVL (cm)	TVL(cm)	MFP(cm)
0.1218	3,2342E-24	4,7862E-25	6,76	3,13E+23	2,88	9,56	4,15
0.2447	2,8241E-24	3,8206E-25	7,39	3,42E+23	3,29	10,94	4,75
0.3443	2,3117E-24	3,3677E-25	6,86	3,18E+23	4,02	13,37	5,81
0.7789	1,5165E-24	2,3827E-25	6,36	2,95E+23	6,13	20,38	8,85
0.964	1,7182E-24	2,1541E-25	7,98	3,69E+23	5,41	17,99	7,81
1.408	1,1375E-24	1,7793E-25	6,39	2,96E+23	8,18	27,17	11,80
$Li_2B_4O_7$:Gd1							
Enerji (MeV)	σ_a	σ_e	Z_{eff}	N_{eff}	HVL (cm)	TVL (cm)	MFP (cm)
0.1218	3,4870E-24	4,8415E-25	7,20	3,30E+23	2,74	9,11	3,96
0.2447	1,7604E-24	3,8289E-25	4,60	2,11E+23	5,43	18,04	7,84
0.3443	2,2184E-24	3,3711E-25	6,58	3,02E+23	4,31	14,32	6,22
0.7789	1,6478E-24	2,3832E-25	6,91	3,17E+23	5,80	19,28	8,37
0.964	1,5206E-24	2,1544E-25	7,06	3,24E+23	6,29	20,89	9,07
1.408	9,6112E-25	1,7795E-25	5,40	2,48E+23	9,95	33,05	14,35

At low photon energies (0.1218 MeV), the Gd-doped sample exhibited slightly higher atomic cross-sections than the pure sample. In addition, an increase in the effective electron density was observed in the doped material, indicating more available electrons for photon interaction.

The effective atomic number values also reflect the influence of Gd. At 0.1218 MeV, Zeff increases from 6.76 in the undoped sample to 7.20 in the Gd-doped one. The enhancement in Zeff is most noticeable at low energies where photoelectric interaction is dominant, aligning with the expected behavior due to gadolinium's high atomic number (Z = 64).

A comparison of shielding effectiveness between the samples reveals significant improvements with Gd addition. The half-value layer decreased from 2.88 cm in the undoped sample to 2.74 cm in the Gd-doped sample at 0.1218 MeV. Similarly, the mean free path also showed a reduction, implying increased attenuation efficiency in the doped sample. At higher energies (e.g., 1.408 MeV), both materials show reduced attenuation performance due to the dominance of Compton scattering and the reduced photoelectric cross-section.

Conclusions

This study investigates gamma-ray interaction parameters of Li2B4O7 doped with the rare earth element Gd. For this purpose, samples were prepared using the solid-state synthesis method. 1% doping rates are used for Gd. The synthesized pellets were used to determine the samples' linear and mass attenuation coefficients in the energy range of 0.1218 to 1.408 MeV. The results were compared with theoretical XCOM values, and agreement was observed. Even though the Gd has high atomic number, its effect is limeted in every energy zone. It was observed that the Gd doping had little effect on the mass attenuation value at all energy values.

The enhancement in attenuation capability provided by Gd doping is consistent at photon energies below 0.2 MeV. This is primarily attributed to the increased Zeff and Neff, which directly influence photon interaction probabilities. While the advantage is more significant at low energies, due to the dominance of the photoelectric effect, improvements persist throughout the measured spectrum.

These results suggest that $Li_2B_4O_7$: 1%Gd is a more effective photon attenuator than pure $Li_2B_4O_7$, below 0.2 MeV energy gamma ray fields. Therefore, Gd-doped lithium tetraborate may be considered a promising candidate material for use in radiation shielding applications and low-energy gamma detectors. Moreover It is expected that the luminance properties of the lithium tetraborate are improved, but this has not been investigated yet.

Conflicts of Interest

There are no conflicts of interest in this work

REFERENCES

[1] Bhalla A. S., Cross L. E., Whatmore R. W., Pyroelectric and piezoelectric properties of lithium tetraborate single crystal, *Japanese Journal of Applied Physics*, 24(S2) (1985) 727.

[2] Adamiv V. T., Burak Y. V., Wooten D. J., McClory J., Petrosky J., Ketsman I., Xiao J., Losovyj Y. B., Dowben P. A., The electronic structure and secondary pyroelectric properties of lithium tetraborate, *Materials*, 3(9) (2010) 4550–4579.

[3] Ketsman I., Wooten D., Xiao J., Losovyj Y. B., Burak Y. V., Adamiv V. T., Sokolov A., Petrosky J., McClory J., Dowben P. A., The off-axis pyroelectric effect observed for lithium tetraborate, *Physics Letters A*, 374(6) (2010) 891–895.

[4] Marzouk Z. G., Dhingra A., Burak Y., Adamiv V., Teslyuk I., Dowben P. A., Long carrier lifetimes in crystalline lithium tetraborate, *Materials Letters*, 297 (2021) 129978.

[5] Zadneprovski B. I., Eremin N. V., Paskhalov A. A., New inorganic scintillators on the basis of LBO glass for neutron registration, *Functional Materials*, 12(2) (2005) 261–268.

[6] Kindrat I. I., Padlyak B. V., Drzewiecki A., Adamiv V. T., Teslyuk I. M., Influence of Ag co-activation on the Dy^{3+} luminescence in lithium tetraborate glasses, *Materials Research Bulletin*, 179 (2024) 112979.

[7] Lucas J., Lucas P., Mercier T. L., Rollat A., Davenport W. G., Rare earths: Science, technology, production and use, *Elsevier*, (2014).

[8] Kindrat I. I., Padlyak B. V., Drzewiecki A., Teslyuk I. M., Adamiv V. T., The impact of silver codoping on Tb^{3+} luminescence in lithium tetraborate glasses, *Luminescence*, 40(1) (2025) e70074.

[9] Ullah B., Kakakhel M. B., Ur Rehman S., Siddique M. T., Munir M., Ahmad K., Mahmood M. M., Wazir-ud-Din M., Anjum I., Synthesis and dosimetric characterization of lithium tetraborate ($Li_2B_4O_7$:Cu,Ag) thermoluminescent dosimeter with improved reproducibility and reusability, *Radiation Physics and Chemistry*, 220 (2024) 111704.

[10] Echeverria E., McClory J., Samson L., Shene K., Colón Santana J. A., Burak Y., Adamiv V., Teslyuk I., Wang L., Mei W.-N., Nelson K. A., McGregor D. S., Dowben P. A., Ilie C. C., Petrosky J., Dhingra A., Lithium tetraborate as a neutron scintillation detector: A review, *Crystals*, 14(3) (2024) 229.

[11] Padlyak B. V., Kindrat I. I., Adamiv V. T., Teslyuk I. M., Drzewiecki A., Spectroscopic properties and luminescence of the lithium tetraborate glasses co-doped with manganese and europium, *Optical Materials*, 154 (2024) 115782.

[12] Sai Dinesh P., Kumar M., Ratnakaram Y. C., Impact of modifiers on structural and optical properties of Dy^{3+}-doped lithium tetraborate glasses for W-LED applications, *Infrared Physics & Technology*, 136 (2024) 105029.

[13] Kouri M. A., Polychronidou K., Loukas G., Megapanou A., Vagena I.-A., Gerardos A. M., Spyratou E., Efstathopoulos E. P., Consolidation of gold and gadolinium nanoparticles: An extra step towards improving cancer imaging and therapy, *Journal of Nanotheranostics*, 4(2) (2023) 127–149.

[14] Vladimir D. R., Grinev B. V., Pirogov E. N., Onyshchenko G. M., Ivanov A. I., Valeriy G. B., Konstantin A. K., Sergiy A. K., Use of gadolinium oxyorthosilicate scintillators in X-ray radiometers, *Optical Engineering*, 44(1) (2005) 016403.

[15] Raymond K. N., Pierre V. C., Next generation, high relaxivity gadolinium MRI agents, *Bioconjugate Chemistry*, 16(1) (2005) 3–8.

[16] Gulbicim H., Akan H., Tufan M. C., Determination of X-ray photon absorption properties of some human tissues and organs using Monte Carlo method, *Indian Journal of Pure & Applied Physics*, 63(2) (2025) 132–143.

[17] Gülbiçim H., Tufan M. Ç., Türkan M. N., The investigation of vermiculite as an alternating shielding material for gamma rays, *Radiation Physics and Chemistry*, 130 (2017) 112–117.

[18] Zali V. S., Jahanbakhsh O., Ahadzadeh I., Preparation and evaluation of gamma shielding properties of silicon-based composites doped with WO_3 micro- and nanoparticles, *Radiation Physics and Chemistry*, 197 (2022) 110150.

[19] Alomari A. H., BaO-doped Na_2O–CaO–P_2O_5 bioactive glasses: A closer look at radiation attenuation properties for medical applications, *Radiation Physics and Chemistry*, 223 (2024) 112019.

[20] Akkurt I., El-Khayatt A. M., Effective atomic number and electron density of marble concrete, *Journal of Radioanalytical and Nuclear Chemistry*, 295(1) (2013) 633–638.

[21] Prasad S. G., Parthasaradhi K., Bloomer W. D., Effective atomic numbers for photoabsorption in alloys in the energy region of absorption edges, *Radiation Physics and Chemistry*, 53(4) (1998) 449–453.

[22] Berger M. J., Seltzer S. M., Chang J., Coursey J. S., Sukumar R., Zucker D. S., Olsen K., XCOM: Photon cross sections database, *National Institute of Standards and Technology*, (2010).